Glycan-Targeted Virus-like Nanoparticles for Photodynamic Therapy

Jin-Kyu Rhee, Michael Baksh, Corwin Nycholat, James C. Paulson, Hiroaki Kitagishi,* and M.G. Finn*

Details of Synthesis and Characterization

Synthetic procedures for zinc porphyrin **2** are summarized in Figure 1 (reproduced as Figure S1 below for convenience).
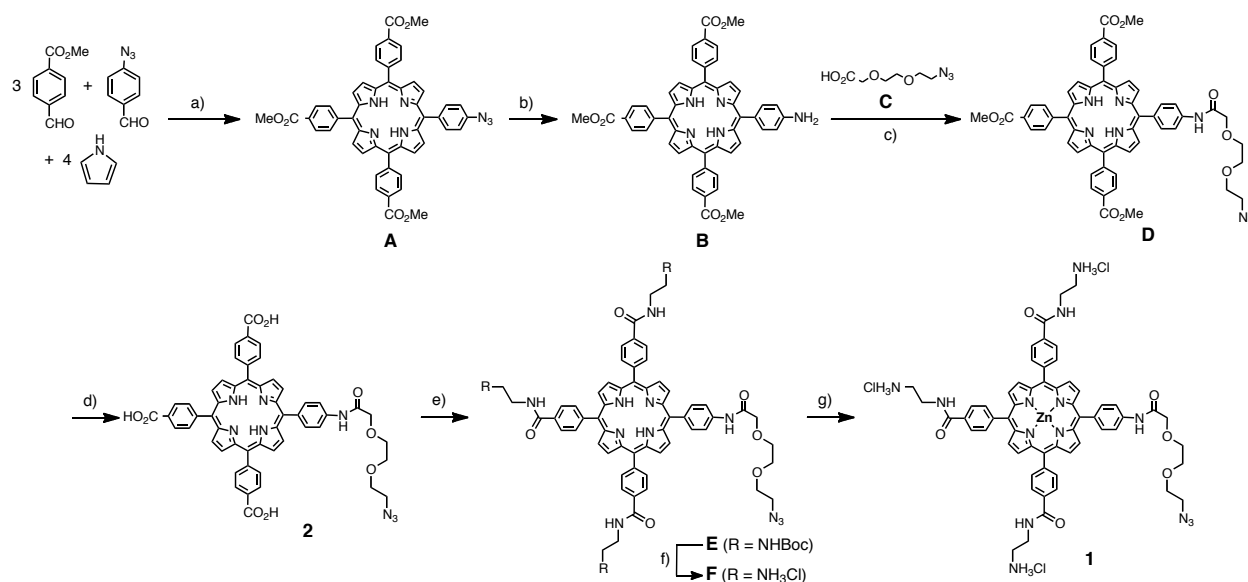

Figure S1. Synthesis of azide-tailed porphyrins. a) BF$_3$•Et$_2$O, CH$_2$Cl$_2$, 8%; b) Na$_2$S, CH$_3$Cl/MeOH, reflux, 70%; c) EDC, HOBt, Et$_3$N, CH$_2$Cl$_2$, 74%; d) NaOH, H$_2$O, THF, 96%; e) BocNH(CH$_2$)$_2$NH$_2$, EDC, HOBt, Et$_3$N, DMF, 54%; f) TFA, CH$_2$Cl$_2$, ion exchange (Cl$^-$ form), 90%; g) ZnO, H$_2$O/MeOH, 86%.

Intermediate A (by the Lindsely procedure[1]): 4-azidobenzaldehyde[2] (0.37 g, 2.5 mmol), 4-carboxymethylbenzaldehyde (1.23 g, 7.5 mmol), and pyrrole (0.66 mL, 10 mmol) were dissolved in CH$_2$Cl$_2$ (500 mL). After the solution was purged with N$_2$, BF$_3$ etherate (0.17 mL, 1.3 mmol) was added and the solution was stirred in the dark for 90 min at room temperature. *p*-Chloranil (2.0 g, 8.1 mmol) was added, and the mixture was stirred overnight. The solvent was evaporated and the residue was purified twice by silica gel column chromatography, eluting with CH$_2$Cl$_2$. The resulting purple solid was dissolved in a minimum amount of CH$_2$Cl$_2$ and re-precipitated by addition of hexane. The purple solid was collected and dried to give **A** (171 mg, 8%). ^{1}H NMR (200 MHz, CDCl$_3$) δ 8.84-8.76 (m, 8H), 8.46 (d, 6H, *J* = 8.6 Hz), 8.30 (d, 6H, *J* = 8.6 Hz), 8.19

[1] Lindsey, J.S.; Hsu, H.C.; Schreiman, I.C. *Tetrahedron Lett*. **1986**, *27*, 4969-4970.

[2] Walton, R.; Lahti, P. M. *Synth*. *Commun*. **1998**, *28*, 1087-1092.

(d, 2H, J = 8.6 Hz), 7.44 (d, 2H, J = 8.6 Hz), 4.12 (s, 9H), -2.71 (bs, 2H); MALDI-TOF MS (dithranol matrix) m/z 802.18 $(M - N_2 + H)^+$, calcd for $C_{50}H_{36}N_5O_6$ 802.27.

Intermediate B: Compound **A** (150 mg, 0.18 mmol) and anhydrous sodium sulfide (150 mg, 0.19 mmol) were dissolved in 1:1 CH_3Cl:MeOH (100 mL). The reaction mixture was refluxed in the dark for 4 h. After the solution was cooled to room temperature, the mixture was washed with brine and H_2O. The organic phase was separated, dried over Na_2SO_4, and evaporated. The residue was purified by silica gel chromatography eluting with 20:1 CH_2Cl_2:acetone. The resulting purple solid was dissolved in a minimum amount of CH_2Cl_2 and re-precipitated by addition of hexane. Compound **B** was obtained as a purple solid (100 mg, 70%). ^{1}H NMR (200 MHz, CDCl$_3$) δ 9.00 (d, 2H, J = 4.8 Hz), 8.82 (d, 2H, J = 4.8 Hz), 8.46 (d, 6H, J = 8.0 Hz), 8.31 (d, 6H, J = 8.0 Hz), 7.98 (d, 2H, J = 8.0 Hz), 7.00 (d, 2H, J = 8.0 Hz), 4.13 (s, 9H), -2.71 (bs, 2H); MALDI-TOF MS (dithranol matrix) m/z 804.79 $(M + H)^+$, calcd for $C_{50}H_{38}N_5O_6$ 804.87.

Intermediate D: Compound **B** (164 mg, 0.20 mmol) and 3,6-dioxa-8-azideoctanoic acid[3] (**C**, 150 mg, 0.79 mmol) were dissolved in dry CH_2Cl_2 (50 mL) and cooled in an iced bath under N_2 atmosphere. To this solution were added EDC hydrochloride (150 mg, 0.78 mmol), HOBt (107 mg, 0.79 mmol), and triethylamine (320 mg, 3.2 mmol), and the solution was stirred at room temperature in the dark. After 4 h, the same amounts of EDC hydrochloride, HOBt, and triethylamine were again added to the solution. After stirring overnight, the solvent was washed with H_2O, the organic phase was separated and dried over Na_2SO_4, and the solvent was evaporated. The residue was purified by silica gel chromatography eluting with 20:1 CH_2Cl_2:acetone. The resulting purple solid was dissolved in a minimum amount of CH_2Cl_2 and re-precipitated by addition of hexane. Compound **D** was obtained as a purple solid (145 mg, 74%). ^{1}H NMR (200 MHz, CDCl$_3$) δ 9.02 (bs, 1H), 8.95 (d, 2H, J = 4.8 Hz), 8.90-8.75 (m, 6H), 8.47 (d, 6H, J = 8.0 Hz), 8.32 (d, 6H, J = 8.0 Hz), 8.23 (d, 2H, J = 8.0 Hz), 8.05 (d, 2H, J = 8.0 Hz), 4.32 (s, 2H), 4.13 (s, 9H), 3.94-3.81 (m, 6H), 3.53 (t, 2H, J = 4.8 Hz), -2.77 (bs, 2H); MALDI-TOF MS (dithranol) m/z 975.64 $(M + H)^+$, calcd for $C_{56}H_{46}N_8O_9$ 975.01.

Compound 2: To a solution of **D** (130 mg, 0.13 mmol) in THF (20 mL) was added 0.1 M NaOH (20 mL). After the solution was stirred for 4 h at room temperature, the THF in the mixture was removed by rotary evaporation. The aqueous residue was acidified to pH 1 with aqueous HCl and cooled in an ice bath. The dark purple precipitate was collected and dried to give **2** (120 mg, 96%). ^{1}H NMR (200 MHz, DMSO-d_6) δ 10.15 (bs, 1H), 8.90-8.83 (m, 8H), 8.37 (d, 6H, J = 8.0 Hz), 8.31 (d, 6H, J = 8.0 Hz), 8.16 (d, 2H, J = 8.0 Hz), 8.10 (d, 2H, J = 8.0 Hz), 4.26 (s, 2H), 3.80-3.67 (m, 6H), 3.47 (t, 2H, J = 4.8 Hz), -2.95 (bs, 2H); MALDI-TOF MS (dithranol) m/z 933.91 $(M + H)^+$, calcd for $C_{53}H_{41}N_8O_9$ 933.94.

Intermediate E: Compound **2** (170 mg, 0.18 mmol) and *N*-Boc-ethylenediamine (**11**, 350 mg, 2.2 mmol) were dissolved in DMF (50 mL). The solution was cooled in an ice bath under N_2 atmosphere. To the solution were added EDC hydrochloride (420 mg, 2.2 x 10^{-3} mol), HOBt

---

[3] Clave, G.; Boutal, H.; Hoang, A.; Perraut, F.; Volland, H.; Renard, P. Y.; Romieu, A. *Org. Biomol. Chem.* **2008**, *6*, 3065-3078.

(297 mg, 2.2 x 10^{-3} mol), and triethylamine (0.92 g, 9.1 x 10^{-3} mol). The solution was stirred at room temperature in the dark. After 4 h, the same amounts of EDC hydrochloride, HOBt, and triethylamine were further added to the solution. After the solution was stirred overnight, the solvent was diluted with 100 mL of CH_2Cl_2 and the mixture was washed with H_2O. The organic phase was separated, dried with Na_2SO_4, and the solvent was evaporated. The residue was purified by silica gel chromatography with CH_2Cl_2/MeOH = 20/1 (v/v). The resulting purple solid was dissolved in a minimum amount of CH_2Cl_2 and re-precipitated by addition of hexane to give **E** (132 mg, 54%). ^{1}H NMR (200 MHz, CDCl$_3$) δ 8.99 (bs, 1H), 8.86 (d, 2H, J = 4.8 Hz), 8.78-8.74 (m, 6H), 8.22 (d, 6H, J = 8.0 Hz), 8.18 (d, 6H, J = 8.0 Hz), 8.12 (d, 2H, J = 8.0 Hz), 7.97 (d, 2H, J = 8.0 Hz), 7.80 (bs, 3H), 5.28 (bs, 3H), 4.29 (s, 2H), 3.89-3.75 (m, 12H), 3.56-3.27 (m, 8H), 1.49 (s, 27H), -2.87 (bs, 2H); MALDI-TOF MS (dithranol) m/z 1358.18 (M)$^+$, calcd for $C_{74}H_{82}N_{14}O_{12}$ 1359.53.

Intermediate F: Compound **E** (130 mg, 0.095 mmol) was dissolved in CH_2Cl_2 (50 mL); the solution was cooled in an iced bath and treated with trifluoroacetic acid (10 mL). After stirring for 4 h at room temperature, the solvent was evaporated and the residue was dissolved in a minimum amount of MeOH. The addition of diethyl ether caused the crude product to precipitate as a dark purple solid. The solid was collected, dissolved in H_2O, and the aqueous solution was passed through ion-exchange resin (Dowex 1x8, Cl$^-$ form). The resulting solution was evaporated to give **F** (100 mg, 90%). ^{1}H NMR (200 MHz, DMSO-d_6) δ 10.15 (bs, 1H), 8.91-8.75 (m, 8H), 8.31-8.21 (m, 12H), 8.19-8.05 (m, 4H), 4.25 (s, 2H), 3.77-3.66 (m, 12H), 3.43 (t, 2H, J = 6.0 Hz), 2.80 (t, 6H, J = 6.0 Hz), -2.95 (bs, 2H); MALDI-TOF MS (dithranol) m/z 1060.08 (M − 3Cl − 2H)$^+$, calcd for $C_{59}H_{59}N_{14}O_6$ 1060.19.

Porphyrin 1: Compound **F** (40 mg, 0.034 mmol) was dissolved in 3:1 H_2O:MeOH (50 mL). To the solution was added zinc oxide (100 mg, 1.2 mmol) and the mixture was refluxed overnight in the dark. After cooling to room temperature, excess ZnO was removed by filtration, and the resulting solution was concentrated and passed through ion-exchange resin (Dowex 1x8, Cl$^-$ form). The solvent was evaporated to give **1** as a dark purple solid (36 mg, 86%). ^{1}H NMR (200 MHz, DMSO-d_6) δ 10.15 (bs, 1H), 8.83-8.70 (m, 8H), 8.41-8.15 (m, 12H), 8.12-8.02 (m, 4H), 4.25 (s, 2H), 3.78-3.65 (m, 12H), 3.47 (t, 2H, J = 6.0 Hz), 2.86 (t, 6H, J = 6.0 Hz); MALDI-TOF MS (dithranol) m/z 1123.65 (M − 3Cl − 2H)$^+$, calcd for $C_{59}H_{57}N_{14}O_6Zn$ 1123.56.

Analyses of the Qβ conjugates. The protein concentrations were determined using the Modified Lowry Protein Assay. Size exclusion chromatography analyses were performed with ÄKTA Explorer (Amersham Pharmacia Biotech) equipment, using superose-6 size-exclusion column. The samples were eluted with 0.1 M potassium phosphate buffer at a flow rate of 0.4 mL/min with detection at 260, 280, and 430 nm. MALDI-TOF MS spectra were recorded on an Applied Biosystems Voyager-DE. The samples for MALDI-TOF MS were prepared as previously described.[5] ICP-OES measurements were obtained on a Varian VISTA ICP-OES spectrometer equipped with Teflon nebulizer and sample uptake tubing. All standards and samples were spiked with yttrium internal standard at 10 ppm to normalize irregularities in nebulization between samples. Zinc concentrations were determined by monitoring three wavelengths and averaging the resulting values. TEM images were acquired with a HP CM100 electron microscope (HP) with 80kV, 1s exposure and Kodak SO163 film on carbon formavor grids

stained with 2% uranyl acetate. DLS measurements were performed on a DynaPro Plate Reader (Wyatt). Before measurement, the protein solutions at a concentration of 0.1 mg/mL were filtered through 0.2-micron filters.

The resulting conjugates were also characterized by MALDI mass spectrometry, which revealed complete labeling of four exposed amines per subunit (three lysines and N-terminus) for **6**, and the subsequent attachment of porphyrin azide in **7** (Figure S2). Integration of the peaks in this latter spectrum shows approximately 45 of the 180 subunits per capsid to bear one porphyrin unit (MW 1125) and approximately three subunits to have two porphyrins attached, assuming equivalent mass spectrometry sensitivity for all of the subunit variants. Attempts to load greater numbers of porphyrins per particle by increasing the reagent concentration or reaction time resulted in poor recoveries of derivatized particles, presumably because of more severe decomposition as porphyrin loading was increased (Figure S2b). MALDI analyses of particles bearing ligands **3** and **4** as well as **1** also showed the expected peaks in approximately the expected relative intensities (Figure S2, particles **8** and **9**). The average number of porphyrin molecules attached to the purified VLPs was measured by determination of the overall concentrations of zinc (by atomic emission spectroscopy) and protein (by modified Lowry assay). In each case, approximately 50 porphyrins were arrayed on the surface of each capsid.
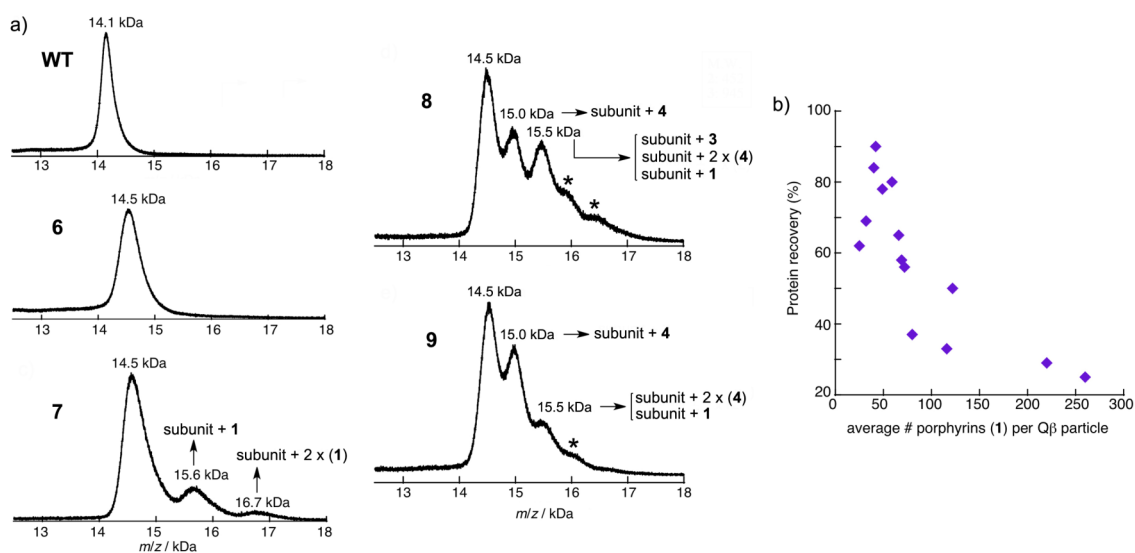

Fig. S2. (a) MALDI analyses of the indicated particles. The term "subunit" means a Qβ coat protein molecule with 4-pentynoate units attached to four surface amine groups (N-terminus, K2, K13, K16). Peaks marked with asterisks are assigned to Qβ subunit protein bearing both porphyrin **1** and a glycan ligand. (b) Relationship of porphyrin loading and particle recovery after CuAAC reaction of **1** with **6**.

Size-exclusion chromatography, dynamic light scattering, and transmission electron microscopy gave data for **7** are shown in Figure S2. The effective site-isolation of VLP surface-confined porphyrins (which gives rise to the sharp Soret peak in Figure 2a) also affected their fluorescence efficiency, the emission intensity of **7** being much greater than that of **1** at a similar porphyrin concentration (Figure S3).
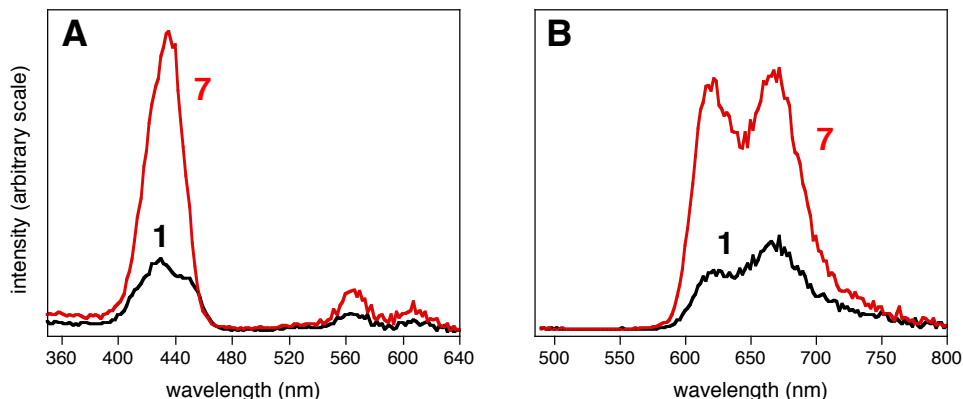
Fig. S3. (A) Excitation (fluorescence monitored at 665 nm) and (B) fluorescence emission spectra (excitation at 418 nm) of zinc porphyrin (**1**) (10 μM) and Qβ particles bearing zinc porphyrin (**7**) (68 nM in particle, 3.4 μM in porphyrin concentration) in 0.1 M potassium phosphate buffer at pH 7.0. The absorbance of these solutions at 418 nm was the same (A_{418} = 0.48) in order to compare the relative fluorescence intensities.

SOSG assay. To detect singlet oxygen in the solution, we used singlet oxygen sensor green (SOSG, Invitrogen). The stock solution of SOSG in methanol (0.5 mM) was added to the aqueous samples in a 96-well plate (200 μL, final concentration 5 μM). The sample solutions were irradiated with a Xenon lamp (Cermax), directed through a water bath to remove heat and ultraviolet light. The resulting SOSG fluorescence was measured on a microplate reader with excitation at 504 nm (Figure S4). The mixture of **7** and SOSG reached a saturated fluorescence intensity after only 60 s irradiation time (Fig. S4a). A direct comparison of **1** and **7** at the same overall porphyrin concentration shows the latter to be significantly more efficient in singlet oxygen generation, presumably because of the lack of porphyrin aggregation (Fig. S4b).
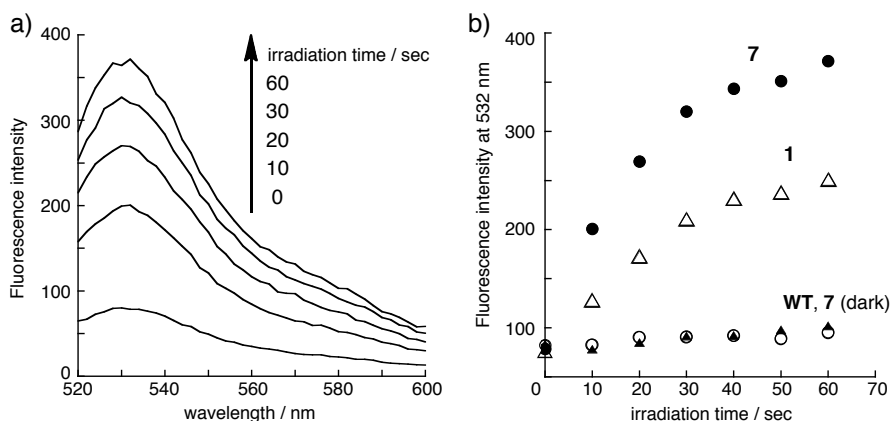

Fig. S4. (a) Fluorescence emission from a mixture of SOSG (5 μM) and **7** (0.66 μM particle; 34 μM porphyrin) in aqueous buffer after the indicated irradiation time. (b) SOSG fluorescence at 532 nm produced by the indicated species: filled circles = **7** (34 μM porphyrin, 0.66 μM VLP); open circles = **7** (reaction vial shielded in foil to block light); open triangles = **1** (40 μM); filled triangles = wild-type VLP (0.60 μM).

Backscattering Interferometry

To verify the attachment of the CD22-binding BPC-sialoside ligand to the VLP surface in **8**, backscattering interferometry measurements were made using small unilamellar vesicles (SUVs) prepared from the membranes of the cells displaying (or lacking) the CD22 receptor. Cells were grown at 37°C and 5% ambient CO_2 to near 100% confluence over three days from initial addition to 175 cm^2-area flasks. Cells were harvested by removing all growth medium from the flask and incubating with 4 mL of Detachin solution for 5 min at 37°C. Incubation buffer (48 mL) was then added to the flask and the contents removed and transferred to two 50 mL centrifuge tubes. The cells and media were centrifuged for 5 min at 300 g to pellet the cells. Following centrifugation, the media was removed from the centrifuge tubes, the cells were re-suspended in 1xPBS, and the cell/PBS suspension re-centrifuged. Cell pellets were rinsed three times in 1xPBS and used immediately. A cell pellet containing approximately $1x10^9$ cells of either type was re-suspended in 20 mL of ice-cold lysis buffer (2.5 mM NaCl, 1 mM Tris, 1x EDTA-free, broad-spectrum protease inhibitors, pH 8.0) and placed on a rotator for 45 minutes at 4°C. The resulting solution was then centrifuged at 40,000 g for 60 min at 4°C. The supernatant was removed and re-suspended in 4 mL of ice-cold 1xPBS and transferred to a 5 mL glass dram vial. The pellet and buffer were then probe-sonicated to clarity in an ice bath and transferred to a 220 nm Millipore Ultrafree-MC centrifuge tube filter. The resulting solutions were centrifuged for 1 h at 16,000 g and 4°C. The solution that passed through the centrifuge tube filter, containing the desired SUVs, was collected and stored at 4°C for no longer than two days before use in BSI analysis.

Ligand binding to the SUVs was accomplished by incubating a fixed amount of SUV suspension with varying concentrations of ligands for 1 hour in the dark at 4°C. Solutions were deposited in the channels of a microfluidic chip for analysis using a backscattering interferometer (BSI). The chip was maintained at 25°C using a feedback-controlled peltier system. The high-contrast interference fringes produced by each sample were generated using a fiber-coupled HeNe laser as a light source and recorded on a CCD camera. Measurements were analyzed using a combination of in-house software, Microsoft Excel, and OriginPro, with the results shown in Figure S5.

A binding constant of 190 ± 60 nM was observed, significantly different from the IC_{50} value of 2.2 μM previously reported for the inhibition of binding of CD22 to immobilized natural sialoside. Particles **8** showed an apparent binding constant of 46 ± 7 μM on a per-ligand basis and 230 ± 35 nM on a per-particle basis (taking into account the average loading of 200 ligands per VLP), strongly suggesting that no avidity or polyvalent effects exist in the interaction of particles with vesicles. Neither **4** nor its polyvalent form **9** showed a detectable interaction with CD22+ membranes by this label-free assay.
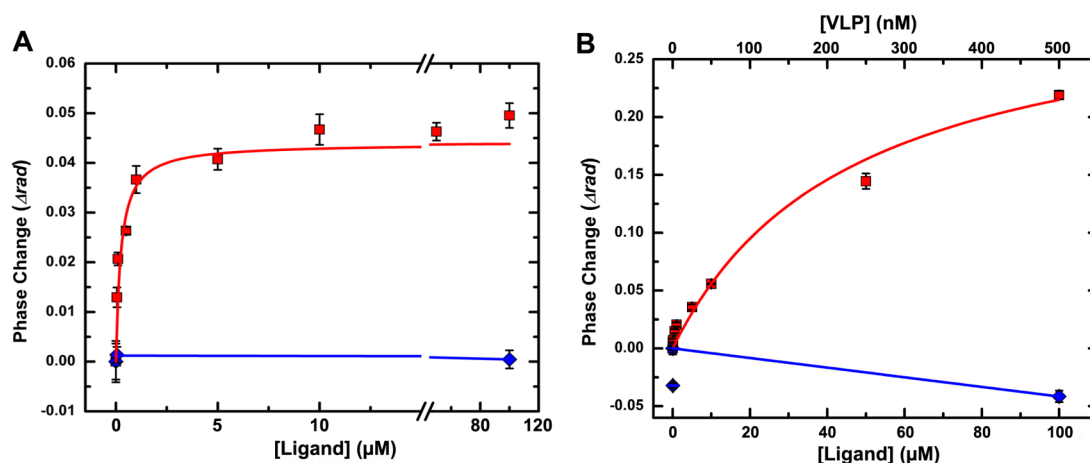
Fig. S5. Representative plots of BSI signal vs. ligand concentration for the determination of binding constants to vesicles prepared by membrane extraction of CD22-positive CHO cells. (A) red = BPC-sialoside ligand **3**; blue = LacNAc **4**. (B) red = particle **8** bearing BPC-sialoside; blue = LacNAc **4**. Ligand concentrations (*x*-axis) refer to the concentrations of glycans. Each data point represents the average of at least four independent measurements; error bars are plus or minus the full value of standard error in each direction.

In vitro photobiological activity.

Figure S6 shows the apparatus used for photochemical experiments. For the studies shown in Figure 4 (uptake of VLPs into cells), the cells were grown on poly-lysine coated glass coverslips, whereas for Figure 6 (cytotoxicity after irradiation), the cells were cultured on sterile plastic 96-well (BD Optilux[TM]) plates. (The only other difference is the omission of the standard phenol red additive in the culture medium of cells being irradiated, since the dye acts as a scavenger of reactive oxygen species.) The Optilux plates were not amenable to high-resolution imaging (oil immersion microscopy) and contributed to background autofluorescence. The difference in surfaces probably contributed to the different morphological appearances of the cells in the two Figures. As expected, the cells showed little or no change when incubated with either buffer or particles (Figure 4), other than differences in fluorescence reflecting differences in particle uptake.

After irradiation, the cell cultures were incubated for 24 h at 37°C in a 5% CO_2 atmosphere, after which the cellular viability was determined by MTT assay.[4] Briefly, after removing the cell medium, 50 μL of MTT solution (1 mg/mL) was added to each well and incubated for 3 h. The resulting formazan crystals were dissolved with 100 μL of 10% SDS in 0.01 M HCl in each well and the absorbance was measured at 595 nm on a microplate reader. For each sample, the cellular viability was calculated from the data of 3 wells (n = 3) and expressed as a percentage, compared with the untreated cells (100%). Figure S7 shows the use of these data (Figure 5A,C) to extract an approximate potency value (represented as IC_{50}) under these conditions. Figure S8 shows a single experiment using an alternative stain for cell death (trypan blue), giving very similar results.

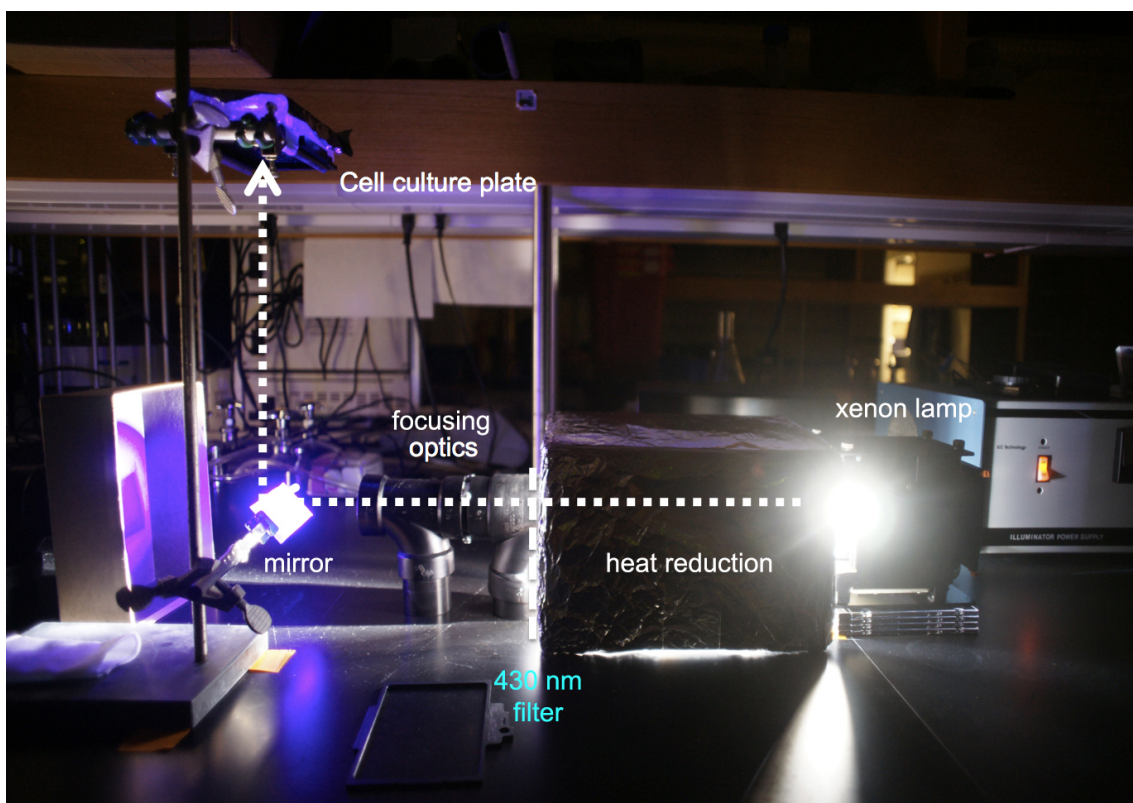[4] Ling, N. R. *J. Immunol. Methods* **1983**, *65*, 1-25.

Figure S6. Apparatus for irradiation of cells for photodynamic therapy measurements. Heat reduction is accomplished by passing the light through a pair of hot mirrors (Newport Corporation) coupled to a pair of focusing optics (convergent lenses, focal length approx. 10 cm). Light wavelengths are controlled using bandpass excitation filters (Chroma Technology Corporation).
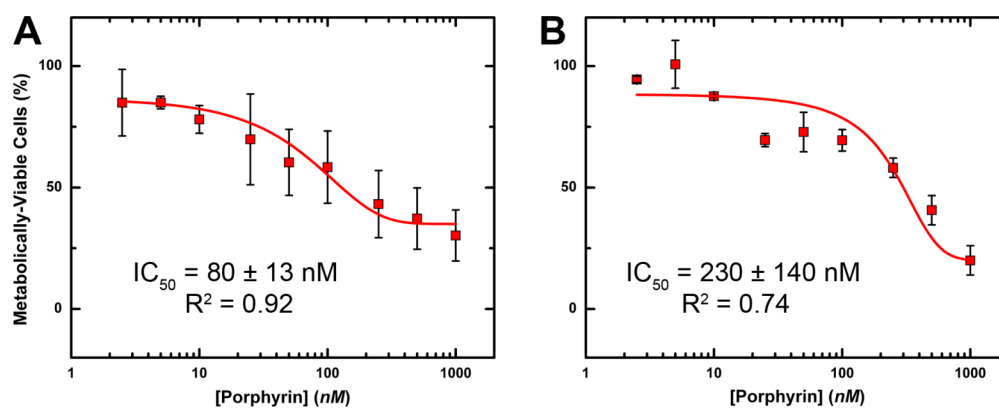

Figure S7. Plots of data shown in Figure 5A and 5C for the photocytotoxic effect of particle **8** at varying concentrations under (A) full-spectrum and (B) filtered (430±10 nm) irradiation. The particle concentrations are approximately 50 times lower than the porphyrin concentrations given, since there are 50±5 porphyrin molecules attached to each particle.

Figure S8. Photo-toxicity results obtained with trypan blue staining. Conditions as in Figures 5C and S7B: 430 nm irradiation, 10 nM particle = 500 nM porphyrin, incubation for 4 h at 37°C followed by washing and irradiation for 90 min. The cells were then immediately stained with trypan blue and the percentage of viable cells was determined.
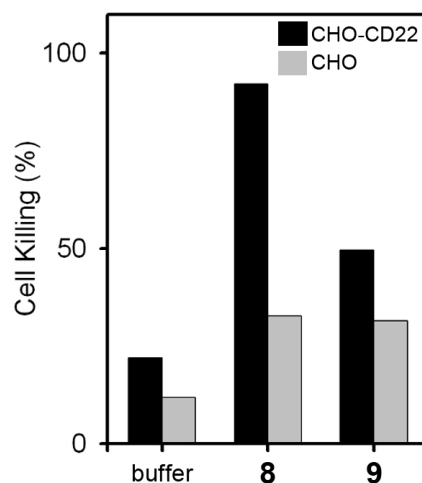
Fluorescence behavior of encapsidated GFP and attached porphyrin

Figure S8 shows fluorescence emission spectra for Qβ virus-like particles encapsidating GFP and/or displaying zinc porphyrin **1**, prepared as described above for **7** and **9**. Excitation of the GFP band at 494 nm resulted in reduced emission from GFP when porphyrin was present (Figure S9A), and excitation of the porphyrin Soret band (along with GFP at this off-maximum wavelength) gave rise to stronger Q-band emission when GFP was present inside the capsid (Figure S9B). While panel B might suggest FRET from GFP to porphyrin, the lack of Q-band emission in panel A does not support such an assignment. For a better behaved (small-molecule donor and acceptor) system on MS2, see Stephanopoulos, N.; Carrico, Z.M.; Francis, M.B. *Angew. Chem. Int. Ed.* **2009**, *48*, 9498-9502.
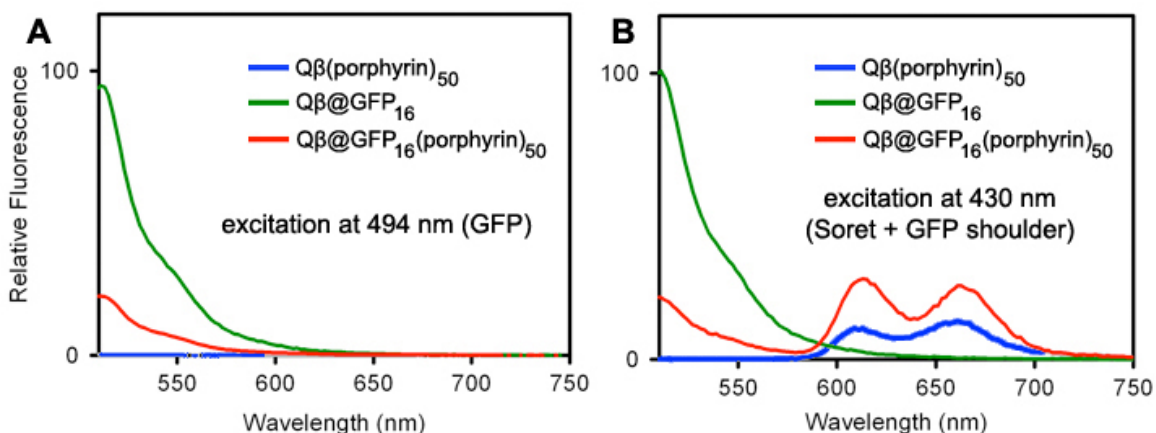

Figure S9. Fluorescence emission spectra of the indicated particles (69 pM in particle; 3.4 μM in porphyrin). (A) excitation at 494 nm (GFP absorbance maximum). (B) excitation at 430 nm (porphyrin Soret band).